BJP BRITISH JOURNAL OF PHARMACOLOGY

BPS BRITISH PHARMACOLOGICAL SOCIETY

British Journal of Pharmacology (2010), 160, 892–906

0007-1188/10
www.brjpharmacol.org

RESEARCH PAPER

Quantitative analysis of neuropeptide Y receptor association with β-arrestin2 measured by bimolecular fluorescence complementation

LE Kilpatrick, SJ Briddon, SJ Hill and ND Holliday

Institute of Cell Signalling, School of Biomedical Sciences, University of Nottingham, Queen's Medical Centre, Nottingham, UK

Background and purpose: β-Arrestins are critical scaffold proteins that shape spatiotemporal signalling from seven transmembrane domain receptors (7TMRs). Here, we study the association between neuropeptide Y (NPY) receptors and β-arrestin2, using bimolecular fluorescence complementation (BiFC) to directly report underlying protein–protein interactions.
Experimental approach: Y1 receptors were tagged with a C-terminal fragment, Yc, of yellow fluorescent protein (YFP), and β-arrestin2 fused with the complementary N-terminal fragment, Yn. After Y receptor–β-arrestin association, YFP fragment refolding to regenerate fluorescence (BiFC) was examined by confocal microscopy in transfected HEK293 cells. Y receptor/β-arrestin2 BiFC responses were also quantified by automated imaging and granularity analysis.
Key results: NPY stimulation promoted association between Y1–Yc and β-arrestin2–Yn, and the specific development of BiFC in intracellular compartments, eliminated when using non-interacting receptor and arrestin mutants. Responses developed irreversibly and were slower than for downstream Y1 receptor–YFP internalization, a consequence of delayed maturation and stability of complemented YFP. However, β-arrestin2 BiFC measurements delivered appropriate ligand pharmacology for both Y1 and Y2 receptors, and demonstrated higher affinity of Y1 compared to Y2 receptors for β-arrestin2. Receptor mutagenesis combined with β-arrestin2 BiFC revealed that alternative arrangements of Ser/Thr residues in the Y1 receptor C tail could support β-arrestin2 association, and that Y2 receptor–β-arrestin2 interaction was enhanced by the intracellular loop mutation H155P.
Conclusions and implications: The BiFC approach quantifies Y receptor ligand pharmacology focused on the β-arrestin2 pathway, and provides insight into mechanisms of β-arrestin2 recruitment by activated and phosphorylated 7TMRs, at the level of protein–protein interaction.
British Journal of Pharmacology (2010) **160,** 892–906; doi:10.1111/j.1476-5381.2010.00676.x; published online 28 April 2010

Keywords: neuropeptide Y; seven transmembrane domain receptor; arrestin; bimolecular fluorescence complementation; automated confocal imaging; desensitization; internalization

Abbreviations: 7TMR, seven transmembrane domain receptor; BIBO3304, (*R*)-*N*$_2$-(diphenylacetyl)-*N*-[(4-(aminocarbonylaminomethyl-)phenyl)methyl]-argininamide; BIBP3226, (*R*)-*N*$_2$-(diphenylacetyl)-*N*-[(4-hydroxyphenyl)methyl]-argininamide; BiFC, bimolecular fluorescence complementation; BRET or FRET, bioluminescence or Förster/fluorescence resonance energy transfer; DMEM, Dulbecco's modified Eagle's medium; ERK, extracellular signal-related kinase; GFP, green fluorescent protein; GR231118 homodimeric, Ile-Glu-Pro-Dpr-Tyr-Arg-Leu-Arg-Tyr-CONH$_2$; GTPγS, guanosine-5′-*O*-(3-thio)triphosphate; NPY, neuropeptide Y; PP, pancreatic polypeptide; PYY, peptide YY; Y1/βarr2, stable co-transfected cells expressing FLAG Y1–Yc and β-arrestin2–Yn; Yc, C-terminal YFP fragment; (c)YFP, (complemented) yellow fluorescent protein; Yn, N-terminal YFP fragment

Correspondence: Dr Nicholas Holliday, Institute of Cell Signalling, School of Biomedical Sciences, University of Nottingham, The Medical School, Queen's Medical Centre, Nottingham NG7 2UH, UK. E-mail: nicholas.holliday@nottingham.ac.uk

Received 29 October 2009; revised 1 December 2009; accepted 14 December 2009

Introduction

β-Arrestins are fundamental regulators of seven transmembrane domain receptor (7TMR) signalling, co-ordinating temporal and spatial response characteristics. They were originally identified as proteins responsible for homologous desensitization, which bind activated and phosphorylated

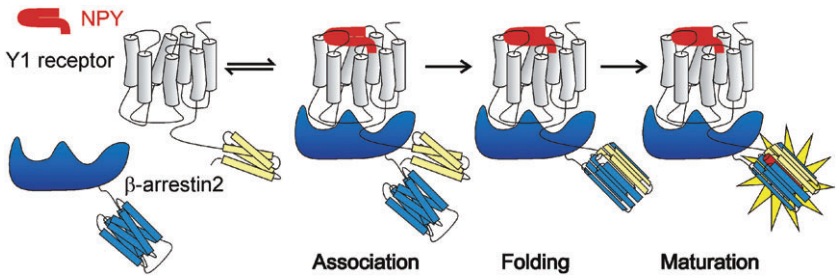

Figure 1 Principle of the 7TMR–β-arrestin2 BiFC assay. Reversible association of β-arrestin2–Yn with NPY-stimulated Y1–Yc receptors promotes stable Yn and Yc fragment refolding. The formation of the YFP β-barrel allows a slower oxidation reaction to generate the internal chromophore, resulting in cYFP fluorescence as an indicator of the interaction.

7TMRs, and so prevent G protein coupling (Gurevich and Gurevich, 2006). However, β-arrestins also act as molecular adaptors to bring many other partners to the 7TMR. For example, β-arrestins recruit second messenger inactivating enzymes, such as phosphodiesterase 4D5 (Perry *et al.*, 2002) or diacylglycerol kinase (Nelson *et al.*, 2007), and association with clathrin and AP-2 drives 7TMR endocytosis (Gurevich and Gurevich, 2006). They also scaffold mitogen-activated protein kinase cascade components, for example, resulting in cytoplasmic extracellular related kinase (ERK1/2) activity retained on endosomal 7TMR–β-arrestin complexes (Gurevich and Gurevich, 2006; Tilley *et al.*, 2009). This diversity in β-arrestin-mediated events is accompanied by the problem of its direction by a given ligand–receptor complex, so that signalling and trafficking can proceed in a specific manner. This is particularly pertinent given the potential to develop 7TMR ligands with biased efficacy towards β-arrestin rather than G protein-based signalling (Azzi *et al.*, 2003; Baker *et al.*, 2003; Zidar *et al.*, 2009). Such problems require techniques which probe the nature of 7TMR association with β-arrestins at the molecular level, and deliver quantitative pharmacology. Current methods based on Förster/fluorescence or bioluminescence resonance energy transfer (FRET/BRET) provide this resolution in living cells (Angers *et al.*, 2000; Berglund *et al.*, 2003; Charest *et al.*, 2005; Hoffmann *et al.*, 2008; Ouedraogo *et al.*, 2008), but they can have a limited dynamic range, and in the case of FRET, the requirement for complex multi-wavelength analysis.

Bimolecular fluorescence complementation (BiFC) is an alternative technique for detecting protein–protein association in live cells (Kerppola, 2008; Rose *et al.*, 2010). The investigated proteins are tagged with split N- and C-terminal fragments of an *Aequorea victoria*-based fluorescent protein, such as the yellow variant (YFP). These fragments (Yn, Yc) are themselves non-fluorescent, but interaction between the tagged proteins brings Yn and Yc together and promotes their refolding into the YFP β-barrel structure. Natural maturation of the chromophore then regenerates YFP fluorescence, giving a simple single-wavelength signal indicating protein–protein association (Figure 1). BiFC can be localized at a subcellular level, and a wide intensity range enhances sensitivity (Kerppola, 2008). Compromises include the slow maturation of complemented YFP (cYFP), which delays the onset of the BiFC response, and BiFC complexes also appear irreversible once formed (Hu *et al.*, 2002). Perhaps because of this, many BiFC studies have focused on stable interactions, for example, between transcription factor dimers (Hu *et al.*, 2002), Gβγ subunits (Mervine *et al.*, 2006) or 7TMR dimers (Briddon *et al.*, 2008; Gandia *et al.*, 2008; Vidi *et al.*, 2008). However, the first fragment refolding step commits a particular interaction to form a BiFC complex, and this is fast enough (half-time of 60 s *in vitro*; Hu *et al.*, 2002) to trap more transient associations typical of signalling proteins (Morell *et al.*, 2007). In the most complete illustration of this possibility, a range of BiFC-based reporters quantified the concerted actions of different compounds on various signalling, mitogenic and apoptotic pathways (MacDonald *et al.*, 2006). This study also confirmed that in principle, the recruitment of β-arrestin2 to the β_2-adrenoceptor could be detected by BiFC reporters (Auld *et al.*, 2006; MacDonald *et al.*, 2006).

Here, we have assessed a quantitative BiFC approach as a means to study the association of β-arrestin2 with two typical rhodopsin-like 7TMRs (Figure 1), the Y1 and Y2 receptors (nomenclature follows Alexander *et al.*, 2009) for neuropeptide Y (NPY) and the related circulating gut hormone peptide YY (PYY). These receptors are involved in the central control of appetite, sympathetic vasoconstriction, gut function and bone development (Michel *et al.*, 1998; Baldock *et al.*, 2007; Karra *et al.*, 2009). Despite shared $G_{i/o}$ protein signalling pathways (Michel *et al.*, 1998), Y1 receptors associate more efficiently with β-arrestin2 than the Y2 subtype, with a corresponding influence on receptor desensitization and internalization (Berglund *et al.*, 2003; Holliday *et al.*, 2005; Ouedraogo *et al.*, 2008). Using the BiFC assay, we have obtained quantitative ligand pharmacology for Y1 receptors and Y2 receptors focused on the specific β-arrestin2 signalling pathway. Moreover, we demonstrate qualitatively distinct effects of receptor mutations which change the ability of β-arrestin2 to recognize activated and phosphorylated 7TMRs.

Methods

Molecular biology

Mutations F64L, M153T, V163A and S175G (numbered as wild-type GFP) were introduced into enhanced YFP cDNA by QuikChange mutagenesis (Stratagene, La Jolla, CA, USA) to generate the venus YFP variant (Nagai *et al.*, 2002). This was the template for PCR-based construction of Yn and Yc fragments 2–154 (N155) and 2–172 (N173), 155–238 (C155) and 173–238 (C173). Each fragment was placed between XhoI and XbaI restriction sites in pcDNA3.1zeo+ (Invitrogen, Paisley, UK),

removing the start methionine and including a stop codon. cDNAs for rat and human Y1 receptors, and the human Y2 receptor, were each PCR amplified to remove start and stop codons, and inserted upstream of the fluorescent protein fragments, before transfer to the vector pCMV FLAG (Stratagene). Receptor fusions were generated which each possessed an N-terminal FLAG epitope (DYKDDDDK), and were joined at the C-terminus to YFP or Yc moieties by the linker sequence LRPLE. FLAG-tagged Y receptor–GFP fusion proteins were constructed in the same manner in the pcDNA4/TO vector (Invitrogen). Amplification of full-length human β-arrestin2 and a truncated bovine β-arrestin1 fragment (319–418) replaced the stop codon with a NotI site to allow in frame cloning upstream of Yn in pcDNA3.1zeo (linker QRPLE). Amino acid substitutions in the Y1 and Y2 receptors were generated by single or sequential QuikChange mutations. Full sequencing confirmed the identity of all receptor and arrestin fusion proteins. Primer sequences are available on request.

Cell culture

HEK293T and 293TR cells (Invitrogen) were cultured in Dulbecco's modified Eagle's medium (DMEM) supplemented with 10% fetal bovine serum and passaged when confluent, by trypsinization (0.25% w/v in Versene, Lonza, Wokingham, UK). Transient and stable transfections were performed using Lipofectamine in Optimem (Invitrogen) according to the manufacturer's instructions. Stable HEK293T β-arrestin2–Yn cell lines were generated by zeocin selection (200 $\mu g \cdot mL^{-1}$) and dilution cloning, screening positive colonies by determining the extent of fluorescence complementation following β-arrestin2–Yc transfection. Y receptor stable mixed populations were then established on a common clonal β-arrestin2–Yn cell background by dual G418 (0.8 $mg \cdot mL^{-1}$) and zeocin resistance. However, the dual cell line expressing the human Y1 receptor required a second round of dilution cloning and selection of an individual colony with adequate receptor expression levels. 293TR Y1–GFP cells were generated as a blasticidin (5 $\mu g \cdot mL^{-1}$)/zeocin resistant mixed population after transfection of the pcDNA4/TO Y1–GFP constructs. These cells, which also express the tetracycline repressor protein, allowed inducible expression of the Y1 receptor–GFP fusion protein after tetracycline treatment (1 $\mu g \cdot mL^{-1}$, 18–21 h before experiments). Stable transfected cell lines were maintained in low levels of blasticidin (5 $\mu g \cdot mL^{-1}$), zeocin (50 $\mu g \cdot mL^{-1}$) or G418 (0.1 $mg \cdot mL^{-1}$) as appropriate to ensure continued selection pressure.

[^{125}I]PYY binding experiments

Membranes were freshly prepared from Y receptor cell lines by two cycles of cold homogenization and centrifugation at 40 000× *g*, resuspending the pellet in 25 mM HEPES, 1 mM Na_2EDTA and 0.1 mM 4-(2-aminoethyl) benzenesulphonyl fluoride (pH 7.4). Protein content was determined by Pierce bicinchoninic acid assay (Fisher, Loughborough, UK). Competition binding assays were performed for 2 h at 21°C in buffer (25 mM HEPES, 2.5 mM $CaCl_2$, 1.0 mM $MgCl_2$, 0.1% bovine serum albumin, 0.1 $mg \cdot mL^{-1}$ bacitracin; pH 7.4) and increasing concentrations of unlabelled ligands (0.1 pM–1 μM, duplicate), using appropriate radioligand conditions for Y1 receptors (15 pM [^{125}I]PYY, 20–40 $ng \cdot \mu L^{-1}$ membrane protein) or the Y2 subtype (10 pM [^{125}I]PYY, 2–4 $ng \cdot \mu L^{-1}$ membrane protein). GTPγS displacements also included 30 $\mu g \cdot mL^{-1}$ saponin in the assay buffer. Membrane-bound radioligand was separated by filtration through Whatman GF/B filters soaked in 0.3% polyethyleneimine on a Brandel cell harvester (Alpha Biotech, London, UK), and retained radioactivity was quantified using a gamma-counter (Packard Cobra II, PerkinElmer, Waltham, MA, USA). Non-specific binding in these experiments comprised less than 5% of total counts.

Confocal microscopy

HEK293T cells were seeded overnight onto 25 mm poly-L-lysine-coated coverslips, and transiently co-transfected with Y1 receptor/β-arrestin cDNAs. Twenty-four hours later, surface Y1 receptors were live labelled with the M2 anti-FLAG antibody as previously described (Holliday *et al*., 2005) prior to stimulation with vehicle or 1 μM NPY for 60 min. Incubations were terminated by fixation, the cells were permeabilized with 0.075% Triton X-100 and the bound M2 antibody was identified by a goat anti-mouse secondary antibody conjugated to Rhodamine Red X. For live studies, cells were grown for 24 h in eight-well Nunc Labtek chamber slides coated with poly-L-lysine (Fisher, Loughborough, UK), and incubated during imaging in Hank's balanced salt solution (with 0.1% bovine serum albumin) in the presence or absence of 1 μM NPY. Confocal images were acquired on a Zeiss LSM 510 laser scanning microscope L87, C2 (Carl Zeiss, Ltd., Welwyn, UK) using a 63× Plan-Apochromat NA 1.4 oil objective, and Ar 488 nm (GFP/YFP) or HeNe 543 nm (Rhodamine Red X) laser lines for excitation. Dual labelled samples were collected in separate scans with emission filters for 505/550 nm band pass (GFP/YFP), together with long pass 560 nm (Rhodamine Red X) and a pinhole diameter of 1 Airy unit set for the longer wavelength. Equivalent laser power and gain settings were used for images of control and agonist-treated cells within the same experiment. Identical linear adjustments to contrast and brightness were made to representative images in the figures for presentation purposes.

Automated imaging of Y receptor–arrestin BiFC responses and Y1 receptor internalization

Dual stable Y receptor/β-arrestin2 BiFC clones, or Y1–YFP cells, were seeded at 50 000 cells per well onto poly-L-lysine-coated 96-well black clear-bottom plates (Costar 3904, Fisher). The next day, the medium was replaced with DMEM/0.1% bovine serum albumin in the presence or absence of antagonist ligands (30 min, 37°C). Agonists were then added for the times indicated (0.1 nM–3 μM, triplicate wells) before incubations were terminated by fixation with 3% paraformaldehyde in phosphate-buffered saline (PBS, 10 min at 21°C). After two PBS washes, cell nuclei were stained for 5 min with the permeable dye H33342 (1 $\mu g \cdot mL^{-1}$ in PBS, Sigma, Poole, UK) and rinsed in PBS. Images (four central sites per well) were acquired automatically on an IX Ultra confocal plate reader (Molecular Devices, Sunnyvale, CA, USA), equipped with a Plan Fluor 40× NA0.6 extra-long working distance objective and 405/488 nm laser lines for H33342 and cYFP excitation respectively. Negative and positive controls (vehicle, 1 μM

NPY) were included on every plate for the purposes of normalization; for mutational studies, these controls were provided by the dual cell line expressing the relevant native Y receptor.

Data analysis

YFP fluorescent images acquired on the IX Ultra were analysed by a granularity algorithm (Transflor, Metaexpress 2.0, Molecular Devices) which identified compartments of at least 3 μm diameter (range set to 3–18 μm, 'vesicles'). Simultaneous classification of smaller compartments (1–3 μm 'pits') provided a data set with equivalent results which, for simplicity, is not shown here. In a given experiment, intensity thresholds for granule classification were set with reference to the negative and positive plate controls. When combined with the nuclear count obtained from the paired H33342 image, granularity analysis provided parameters of vesicle count, area and average intensity per cell, in which each individual data point was obtained from assessment of 12 images (four sites per well in triplicate). Concentration–response curves for different ligands were then normalized as a percentage of the control response (typically 1 μM NPY for the respective native Y receptor), and this allowed pooling of individual experiments. Curves were fitted to the pooled data by non-linear least square regression, and where appropriate multiple comparisons between data groups were assessed for significance by one-way ANOVA and Dunnett's post-test (Graphpad Prism v5.01, San Diego, CA, USA).

Binding pK_i values were estimated from IC_{50} measurements in [^{125}I]PYY competition studies using the Cheng–Prusoff equation. Due to the relatively low levels of receptor expression in Y receptor/β-arrestin2 clones, B_{max} estimates were obtained from homologous PYY displacements according to the equation $B_{max} = TSB \times IC_{50}/[L]$, where TSB is the total specific binding in the absence of agonist, and [L] is the radioligand concentration.

Materials

The enhanced YFP cDNA sequence was kindly provided by Dr F. Ciruela (University of Barcelona, Barcelona, Spain). Molecular biology reagents were purchased from Fermentas (St.Leon-Rot, Germany), Promega (Southampton, UK) or Sigma (Poole, UK). The M2 monoclonal anti-FLAG antibody and secondary antibody conjugates were from Sigma and Invitrogen respectively. [^{125}I]PYY (specific activity 81.4 TBq mmol^{-1}) was provided by PerkinElmer. All non-labelled peptides were purchased from Bachem (St. Helens, UK) and stored as single-use aliquots at –20°C. BIBP3226 was obtained from Sigma, while BIBO3304 was a gift from Boehringer-Ingelheim, GmbH (Biberach, Germany). Cell culture media and selection antibiotics were sourced from Sigma, Lonza (Wokingham, UK) or Invitrogen as appropriate.

Results

NPY Y1 receptor association with β-arrestin2 can be detected by BiFC

We used BiFC fragment pairs based on a rapid folding YFP variant called venus (Nagai *et al.*, 2002), to maximize trapping of agonist-induced Y1 receptor–β-arrestin2 complexes at physiological temperature (37°C). Early optimization suggested that C-terminal tagging of the rat Y1 receptor with Yc (155–238) was most suitable, in combination with β-arrestin2 fused at the C-terminus to Yn (1–173). This overlapping pair (N173:C155) repeats a β-strand (155–172) in both Yn and Yc, as an aid to the refolding process (Hu and Kerppola, 2003). Y1–Yc and βarr2–Yn cDNAs were co-transfected into HEK293 cells, and receptors were identified by live antibody labelling of the N-terminal FLAG epitope (Figure 2). Under control conditions, relatively low levels of cYFP fluorescence were observed, but following 60 min treatment with NPY, there was a marked increase in BiFC. This was located principally in perinuclear intracellular compartments and largely co-localized with receptor immunoreactivity. In contrast, the agonist-induced BiFC response was absent when using a truncated Y1 receptor construct lacking much of the C-terminal tail after the palmitoylation site (ΔY346), or when full-length Y1–Yc was partnered with truncated β-arr1(318–419)–Yn without receptor binding domains (Figure 2). In both these controls, Y1 receptor internalization was also largely prevented.

We derived more quantitative data on the BiFC response by obtaining dual stable clones with Y1–Yc receptors as a mixed population ([^{125}I] PYY B_{max} 350 ± 60 fmol·mg^{-1} membrane protein; n = 4) established on a βarr2–Yn clonal cell line, called Y1/βarr2. The majority of Y1/βarr2 cells responded to NPY stimulation with increased vesicular cYFP fluorescence (see Supporting Information Figure S1). When seeded into 96-well plates, images from these cells could be collected in an automated manner using a confocal plate reader (Figure 3). A granularity algorithm identified the larger BiFC-positive compartments ('vesicles', >3 μm diameter) within every image, and calculated various vesicle parameters normalized to the nuclear count. This unbiased analysis enabled derivation of full ligand concentration–response curves for each parameter, and the calculation of NPY pEC_{50} values (range: 8.51–8.70) for the stimulation of Y1/βarr2 BiFC (Figure 3). In subsequent experiments, vesicle count and area measurements produced similar results to data based on vesicle average intensity, which is presented here.

Kinetics and reversibility of Y1/βarr2 BiFC

cYFP localization patterns observed in Y1/βarr2 cells were similar under control or NPY-treated conditions, with predominant (although not exclusive) intracellular distribution in perinuclear compartments. Thus, the increased vesicular cYFP intensity after agonist stimulation strongly indicated the generation of *de novo* BiFC, rather than trafficking of pre-existing complexes. In order to exclude this second possibility entirely, NPY responses in Y1/β-arr2 cells were compared to the time-profiles of NPY-stimulated Y1 receptor trafficking (Figure 4). Endocytosis assays used HEK293 cells stably transfected with Y1 receptors fused to full-length venus YFP. The granularity algorithm was applied to plate reader Y1–YFP images to detect and quantify internalized receptors (see Supporting Information Figure S2), using the same vesicle diameter constraints applied to BiFC images.

Development of Y1/β-arr2 BiFC in response to 100 nM NPY ($t_{1/2}$ 10.4 ± 1.0 min, n = 3; Figure 4B) was significantly slower

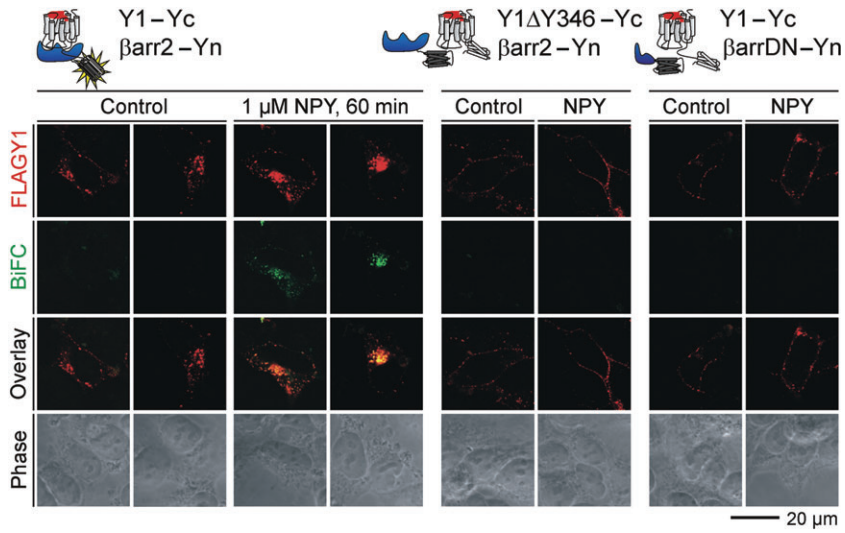

Figure 2 NPY specifically stimulates Y1 receptor–β-arrestin2 BiFC. HEK293 cells were transiently co-transfected with FLAG-tagged Y1 receptor–Yc and β-arrestin–Yn plasmids. Cells were live labelled 24 h later with M2 anti-FLAG antibody before treatment with vehicle or 1 μM NPY for 60 min at 37°C. Following fixation, the M2 antibody was identified in fixed cells by a secondary antibody conjugated to Rhodamine Red X. Images were acquired using a Zeiss LSM510 confocal microscope with laser excitation at 488 nm (cYFP BiFC fluorescence, and phase) or 543 nm (M2 detected FLAG Y1 receptors). Representative images are shown from one of at least three experiments. They illustrate the increase in BiFC fluorescence, co-localized with receptor immunoreactivity, in NPY-stimulated cells co-transfected with Y1–Yc and β-arrestin2–Yn. This response was absent when using either a Y1 receptor–Yc construct lacking the C tail after Tyr346 (ΔY346), or a dominant negative (DN) truncated β-arrestin1(319–418)–Yn.

than for NPY stimulated Y1–YFP internalization ($t_{1/2}$ 2.4 ± 0.3 min, $n = 3$; $P < 0.05$; Figure 4A). Agonist removal by three washes with medium, lasting 1 h in total, led to complete recovery of the Y1–YFP receptor at the cell surface, and associated reversibility of the fluorescence signal in endocytic compartments (Figure 4A; NPY response after washing: 8.3 ± 11.7% ($n = 3$) of control 2 h NPY response). In contrast, Figure 4B shows that NPY-stimulated Y1/β-arr2 BiFC persisted after the same wash protocol (75.4 ± 12.0% of control 2 h NPY response, $n = 3$; $P < 0.05$ compared to Y1–YFP data).

We also considered the effect of using different BiFC fragment pairs on NPY response kinetics (Figure 4C,D). Y1/β-arr2 cells, using the overlapping N173:C155 combination, were compared with two alternative dual clones. These expressed either Y1–Yc (155–238) paired with βarr2–Yn (1–154) (N155:C155, [^{125}I] PYY B_{max} 650 ± 100 fmol·mg^{-1} membrane protein, $n = 4$) or Y1–Yc (173–238) in combination with βarr2–Yn (1–172) (N173:C173; [^{125}I] PYY B_{max} 300 ± 120 fmol·mg^{-1} membrane protein, $n = 3$). Both exhibited slower BiFC responses to 100 nM NPY (N155:C155 $t_{1/2}$ 17.5 ± 2.6 min, $n = 4$; N173:C173 $t_{1/2}$ 20.9 ± 1.7 min, $n = 3$; both $P <$ 0.05 compared to Y1/βarr2 cells, N173:C155). However, as for Y1/βarr2 cells (N173:C155), the NPY-induced BiFC in each case was largely irreversible (Figure 4C,D).

Agonist and antagonist pharmacology

NPY concentration–response curves measured in Y1/βarr2 cells yielded similar potency estimates when incubation times were varied from 15 min to 4 h (pEC_{50} range: 8.39–8.60; $n =$ 3); however, the maximum agonist-induced BiFC response was greatest following incubation times of 1 h or greater. Using 1 h incubation times, comparison of different peptide agonists demonstrated typical Y1 receptor pharmacology for stimulation of Y1/βarr2 BiFC. The endogenous ligands NPY and PYY, and the selective analogue [Leu^{31}, Pro^{34}]NPY were equipotent full agonists (Figure 5). In contrast, the third NPY family member, pancreatic polypeptide (PP), and the metabolite NPY_{3-36} were much less potent. Both the rank order of potency and the actual pEC_{50} values obtained were similar to those measured for stimulation of Y1–YFP endocytosis (Figure 5; Table 1). Moreover, concentration–response curves to the different agonists were not influenced by the use of alternative YFP fragment pairs to generate Y1/βarr2 BiFC (Figure 5; Table 1).

A peptide Y1 receptor antagonist GR231118, reported to increase Y1 receptor internalization (Pheng *et al.*, 2003), was inactive in both Y1–YFP endocytosis and βarr2 BiFC assays (Figure 5). Equally, Y1/βarr2 BiFC was not altered by the non-peptide antagonists BIBP3226 (1 μM yielded –4.5 ± 10.0% of 1 μM NPY response; $n = 4$) or BIBO3304 (at 30 nM: –8.7 ± 7.5% of 1 μM NPY response; $n = 5$). However, 30 min pre-incubation with either BIBP3226 or BIBO3304 resulted in parallel rightward shifts of the NPY concentration–response curves for Y1/βarr2 BiFC, consistent with competitive reversible antagonism (Figure 6). The respective Schild plots yielded pA_2 estimates of 8.0 ± 0.1 for BIBP3226 (slope 1.1 ± 0.1, $n =$ 4) and 9.0 ± 0.1 for BIBO3304 (slope 1.1 ± 0.1, $n = 5$). This functional estimate for BIBO3304 affinity was the same as its pK_i measured in [^{125}I]PYY competition assays in Y1/βarr2 membranes (Table 2). GR231118 also acted as an antagonist in similar pre-incubation experiments (Figure 6C), yielding a pA_2 estimate of 8.6 ± 0.2 ($n = 4$); however, linear GR231118 Schild plots were greater than unity (slope 1.5 ± 0.2).

Stable expression of the human Y1 receptor is more difficult than for its rat orthologue, but we were also able to derive a

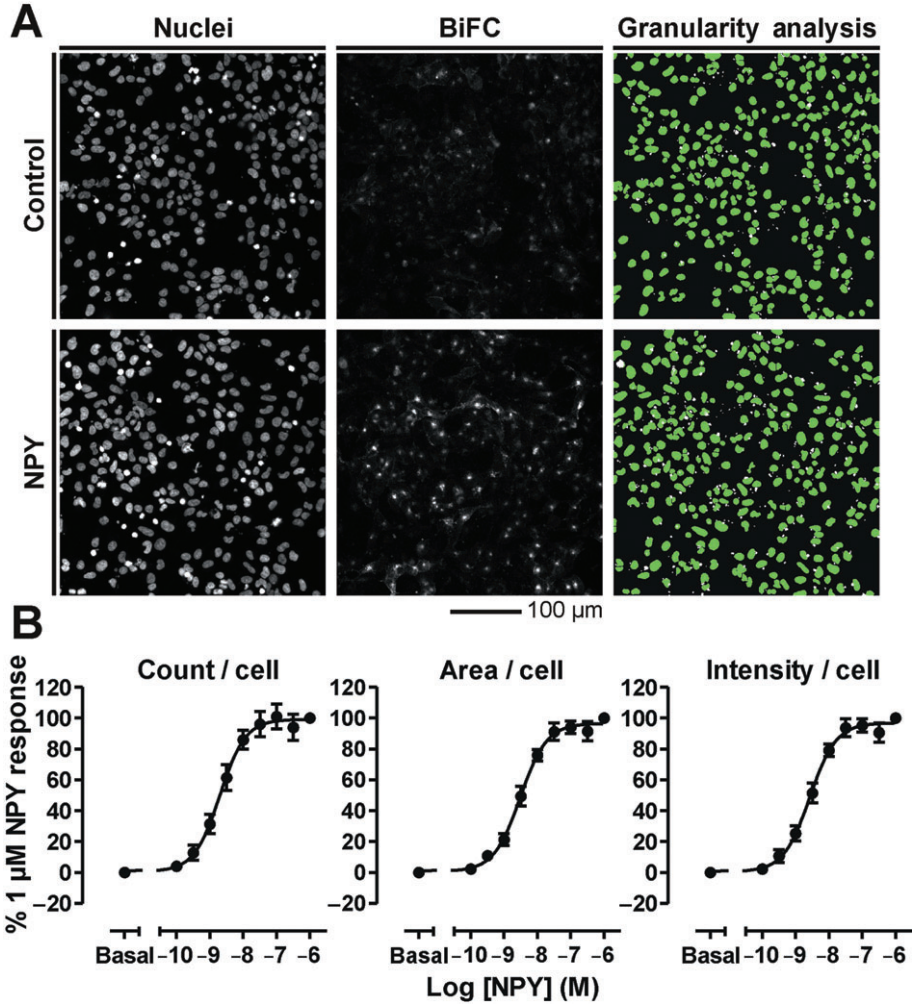

Figure 3 Quantitative analysis of Y1 receptor–β-arrestin2 BiFC. Example images acquired on an IX Ultra plate reader (A) show stable co-transfected Y1/βarr2 cells under control conditions or treated with 1 µM NPY for 60 min (see also Supporting Information Figure S1 for higher resolution). Images of H33342 nuclei staining (left panels) and β-arrestin2 BiFC fluorescence (central panels) were processed by a granularity algorithm with results shown in the right-hand panels. The analysis identified nuclei in green, and BiFC compartments more than 3 µm in diameter (white dots) based on detection thresholds set with reference to the plate controls. In (B), pooled data from the granularity analysis are presented as normalized NPY concentration–response curves (n = 10) for vesicle count/cell (pEC_{50} 8.70 ± 0.09), vesicle area/cell (pEC_{50} 8.51 ± 0.06) and vesicle average intensity/cell (pEC_{50} 8.57 ± 0.05).

dual transfected cell line capable of measuring the association of the human Y1 receptor with β-arrestin2 by BiFC ([^{125}I]PYY B_{max}: 610 ± 20 fmol·mg^{-1}, n = 3). This demonstrated equivalent agonist and BIBO3304 pharmacology for both rat and human Y1 receptor/βarr2 association (Figure 7).

Mutational analysis of Y1 receptor/β-arrestin2 interaction

We examined whether the BiFC assay could quantify the effects of receptor mutation on β-arrestin2 recruitment. Y1/βarr2 responses were compared with those in clones expressing Y1–Yc mutant receptors as a mixed population on the same βarr2–Yn parent cell line. For each experiment, Y1/βarr2 cell controls on the same plate ensured appropriate normalization of the data, and no change in overall subcellular distribution of cYFP complexes was evident with any receptor mutant. We first investigated the effect of Y99A substitution, which prevents NPY binding to the Y1 receptor (Sjodin *et al.*, 2006), and the C tail truncation ΔY346 which prevented βarr2 BiFC in transiently transfected cells (Figure 2). Receptor expression was detected by anti-FLAG labelling in both Y1Y99A/βarr2 and Y1ΔY346/βarr2 cells (data not shown), and by [^{125}I]PYY binding experiments in the Y1ΔY346/βarr2 clone (Table 2). However, both mutations eliminated NPY stimulated BiFC responses measured by granularity analysis (Table 3).

Previous work by our own and other groups has identified a phosphorylated sequence in the Y1 receptor C-terminus (serine 352–serine 362) which is implicated in β-arrestin binding and its functional consequences, such as desensitization of G protein coupling and receptor internalization (Holliday *et al.*, 2005; Ouedraogo *et al.*, 2008). We assessed the relative importance of the six serine/threonine residues within this region by their mutation to alanine, alone or in combination (Figure 8). Mutant Y1 receptors were expressed at a similar level to Y1–Yc in dual βarr2 clones, and displayed

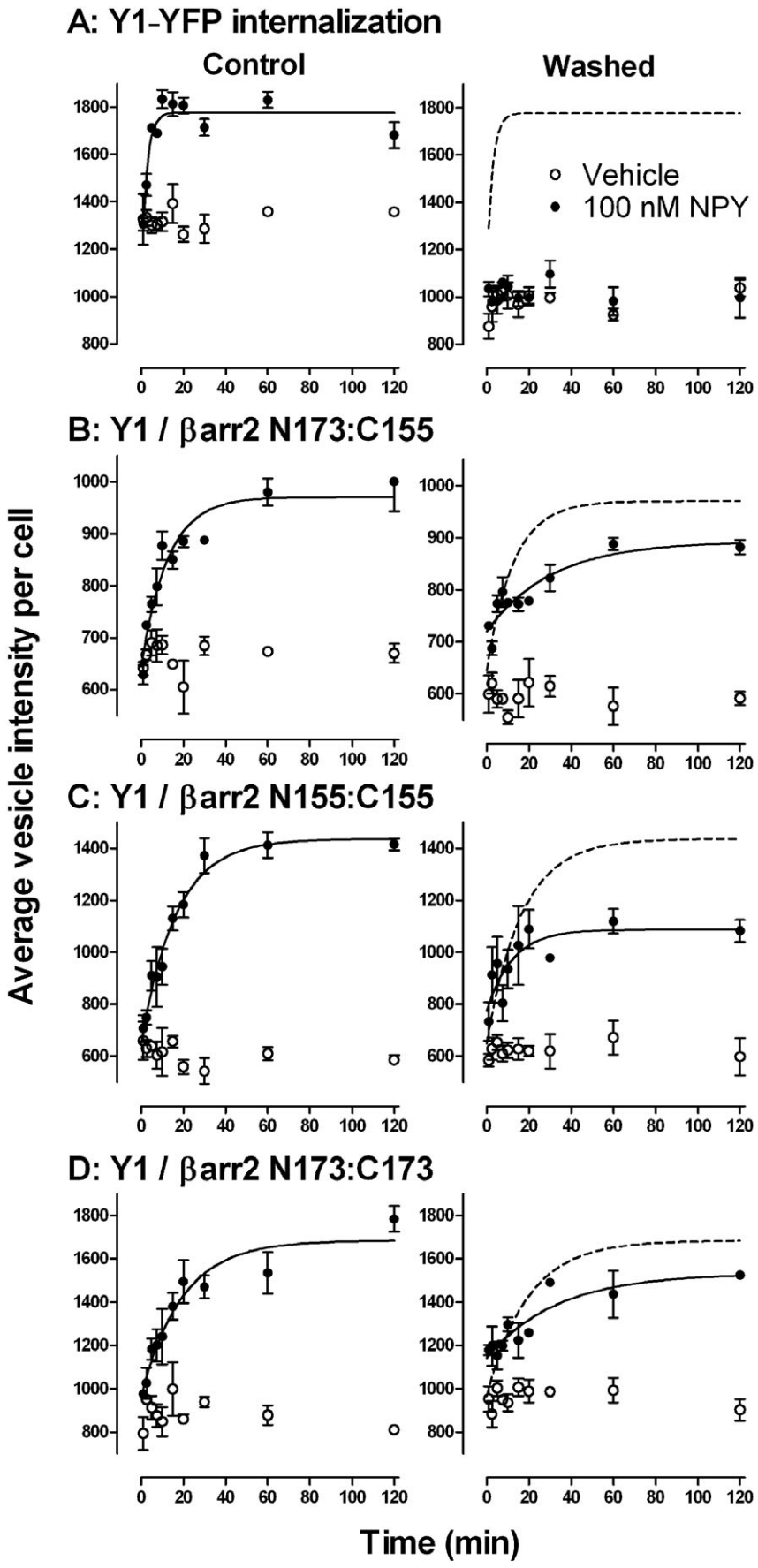
A: Y1-YFP internalization
Control
Washed
Vehicle
100 nM NPY
B: Y1 / βarr2 N173:C155
C: Y1 / βarr2 N155:C155
D: Y1 / βarr2 N173:C173
Average vesicle intensity per cell
Time (min)

Figure 4 Kinetics and reversibility of β-arrestin2 BiFC compared to Y1–YFP internalization. Y1–YFP endocytosis was measured in HEK293 cells using the granularity algorithm (A, see also example in Supporting Information Figure S2). This was compared to the quantified BiFC responses in Y1/βarr2 cells using the N173:C155 fragment pair (B), or alternative stable clones expressing (C) Y1–Yc (155–238) and β-arrestin2–Yn (1–154) (N155:C155) or (D) Y1–Yc (173–238) and β-arrestin2–Yn (1–172) (N173:C173). Single example experiments (from $n = 3$) show a 2 h time-course for vehicle or 100 nM NPY treatment, in which cells were fixed immediately (left-hand graphs, control), or the agonist first removed by three media washes (for 60 min at 37°C, right-hand graphs). Control NPY time-courses were fitted with a one-phase hyperbola which gave individual half-times ($t_{1/2}$) of 1.8 min (A, Y1–YFP), 8.7 min (B, N173:C155), 11.5 min (C, N155:C155) and 13.4 min (D, N173:C173). For comparison, these fits are represented as dotted lines on the right-hand graphs. Pooled $t_{1/2}$ measurements are given in the text.

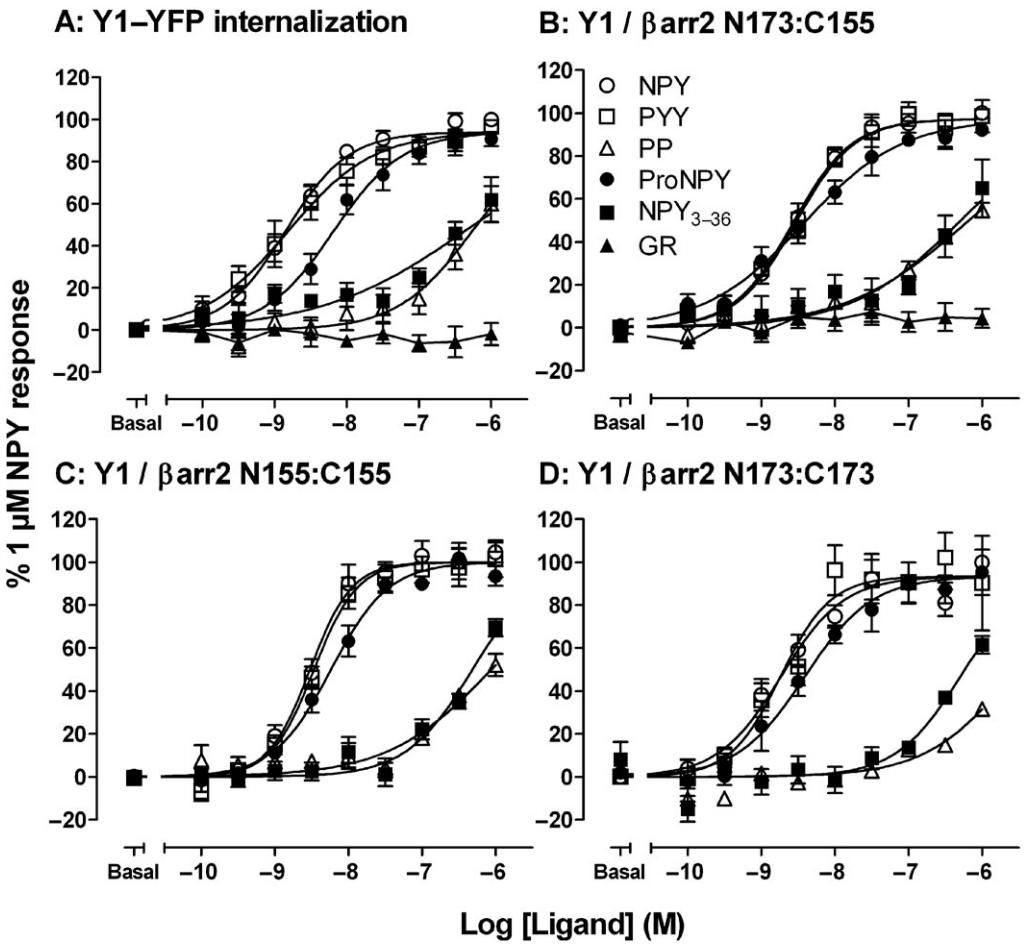

Figure 5 Concentration–response curves for Y1–YFP receptor internalization and Y1 receptor–β-arrestin2 BiFC. Responses to different ligands were measured by granularity analysis applied to automated plate reader images (calculating vesicle average intensity/cell), and normalized to the positive control on each plate (1 μM NPY). Combined data from stably transfected cells are presented for Y1–YFP internalization following 15 min treatment (A, $n = 3–5$), or Y1 receptor–β-arrestin2 BiFC measured at 60 min, using Yn and Yc partners N173:C155 (B, $n = 4–10$), N155: C155 (C, $n = 4–6$) or N173:C173 (D, $n = 2–6$). Peptides examined included [Leu^{31}, Pro^{34}]NPY (ProNPY) and GR231118 (GR, A and B only). Where appropriate, pEC_{50} values from the pooled data are presented in Table 1.

equivalent agonist and antagonist binding affinities in [^{125}I]PYY competition assays. In each case, [^{125}I]PYY binding was also sensitive to GTPγS, an indicator of appropriate G protein coupling (Table 2).

Paired substitution of S352A, T353A (STA) or T356A modestly reduced maximal NPY- and PYY-stimulated Y1/βarr2 BiFC. S359A or the double mutant T361A, S362A (TSA) were individually without effect, but these mutations did significantly enhance the inhibition afforded by either STA or T356A (Figure 8; Table 3). Combinations eliminating 4/6 Ser/Thr residues inhibited maximal agonist-stimulated BiFC by 55–65%, despite preserving T356 in the sequence (STA, TSA mutant) or S352 and T353 (T356A, S359A, TSA mutant). Agonist responses were almost entirely eliminated by mutation of the remaining two serine or threonine residues, either in the Y1 5A mutant (with only T356 still present) or in the Y1 6A construct (Figure 7; Table 3). No phosphorylation site mutation altered the potencies of NPY or PYY BiFC responses, when these could be accurately measured (Figure 8; Table 3).

The 6A mutation was also sufficient to prevent agonist-stimulated Y1 receptor internalization (Figure 9). For example, stimulation of Y1–GFP receptors by NPY (1 μM) led to rapid receptor internalization, while Y16A–GFP receptors did not undergo endocytosis with the same treatment.

Table 1 Agonist potencies and maximum responses for stimulating Y1 receptor internalization and Y1/βarr2 BiFC

Agonist	*Y1–YFP internalization*		*Y1/βarr2 N173:C155*		*Y1/βarr2 N155:C155*		*Y1/βarr2 N173:C173*	
	pEC_{50}	*1 μM (%)*	*pEC_{50}*	*1 μM (%)*	*pEC_{50}*	*1 μM (%)*	*pEC_{50}*	*1 μM (%)*
NPY	8.85 ± 0.07	100	8.57 ± 0.05	100	8.52 ± 0.04	100	8.73 ± 0.09	100
PYY	8.81 ± 0.10	96.6 ± 2.3	8.54 ± 0.06	98.6 ± 7.6	8.47 ± 0.05	101.6 ± 8.5	8.74 ± 0.08	90.3 ± 22.0
ProNPY	8.18 ± 0.08	90.1 ± 7.6	8.43 ± 0.08	93.4 ± 3.1	8.24 ± 0.06	93.5 ± 4.5	8.41 ± 0.10	95.3 ± 10.5
NPY_{3-36}	<7.0	61.8 ± 10.8	<7.0	65.0 ± 13.0	<7.0	69.5 ± 4.0	<7.0	61.6 ± 4.1
PP	<7.0	59.9 ± 8.9	<7.0	54.7 ± 3.4	<7.0	52.1 ± 5.3	<7.0	31.6

pEC_{50} data were obtained from concentration–response curves presented in Figure 5 ($n = 2$–10). N173:C155, N155:C155 and N173:C173 indicate the specific Yn and Yc partners used to generate BiFC responses for each Y1/βarr2 cell line; 1 μM responses to each ligand were expressed as a percentage of the NPY response. ProNPY, [Leu^{31}, Pro^{34}]NPY.

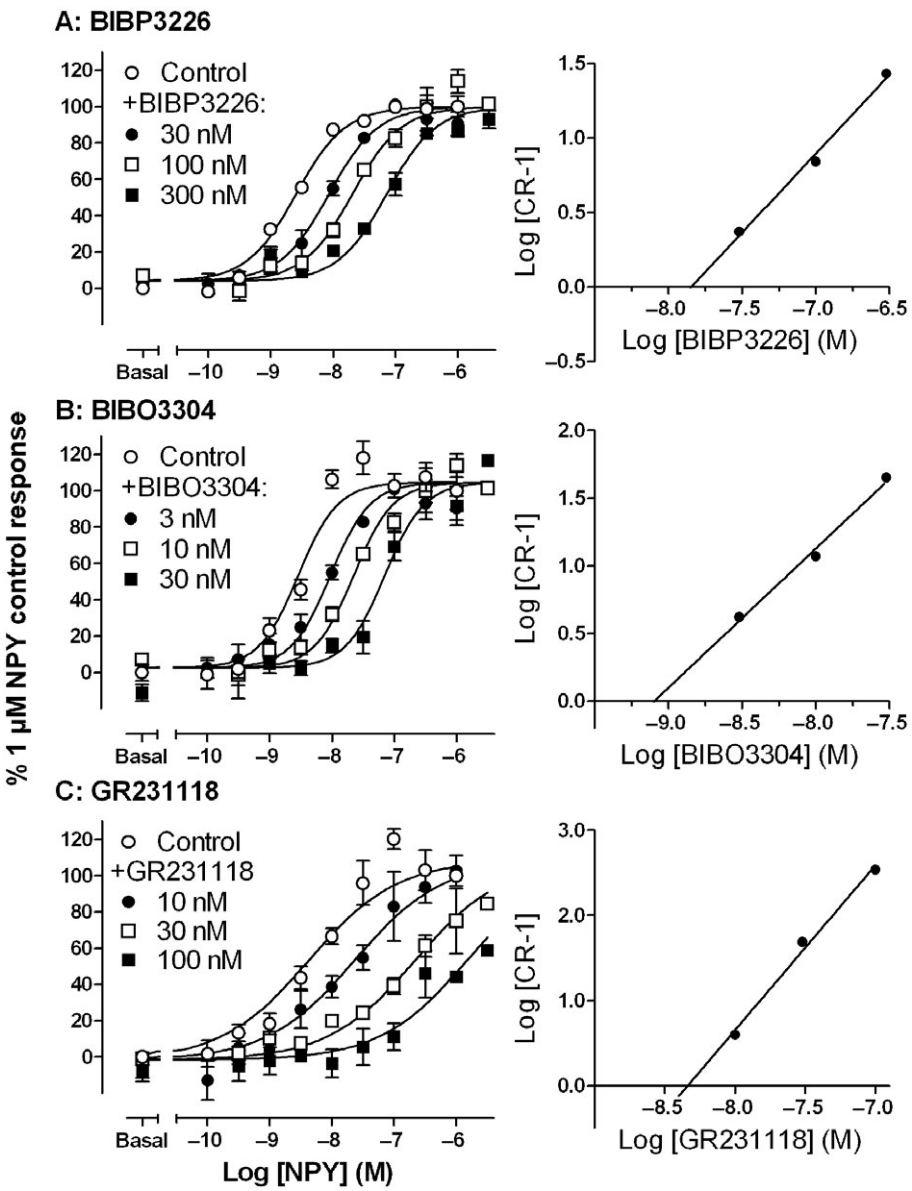

Figure 6 Antagonists inhibit Y1 receptor–β-arrestin2 BiFC. In the example, triplicate experiments shown, Y1/βarr2 cells were pretreated for 30 min with antagonists BIBP3226 (A), BIBO3304 (B) and GR231118 (C) at the concentrations indicated. NPY was then applied for 60 min, before measuring BiFC responses (vesicle average intensity/cell, normalized to control 1 μM NPY in each case). NPY concentration–response curves in the absence or presence of antagonist were fitted (GraphPad Prism) assuming shared minimum, maximum and Hill slope constants. The EC_{50} concentration ratios (CR) were used to construct Schild plots with the following fits for BIBP3326 (pA_2 7.8, slope 1.1), BIBO3304 (pA_2 9.1, slope 1.0) and GR231118 (pA_2 8.3, slope 1.9). Pooled pA_2 values are given in the text.

Table 2 Summary of binding parameters for Y1 and Y2/βarr2 dual clones

Receptor	*PYY*		*BIBO3304*	*GTPγS*	
	pK$_i$	*B$_{max}$ (fmol·mg^{-1})*	*pK$_i$*	*pIC$_{50}$*	*1 μM inhibition (%)*
Y1	9.76 ± 0.10	350 ± 60	9.01 ± 0.12	9.05 ± 0.21	58.6 ± 4.1
Y1 ΔY346	9.59 ± 0.12	980 ± 200	9.03 ± 0.04	8.57 ± 0.04	61.9 ± 8.8
Y1 STA	9.76 ± 0.03	420 ± 70	9.05 ± 0.06	9.00 ± 0.15	61.4 ± 4.0
Y1 T356A	9.65 ± 0.14	570 ± 120	9.08 ± 0.09	8.97 ± 0.17	48.3 ± 4.7
Y1 S359A	9.74 ± 0.08	580 ± 110	9.06 ± 0.08	9.18 ± 0.08	54.7 ± 3.5
Y1 TSA	9.73 ± 0.07	580 ± 20	9.25 ± 0.25	9.40 ± 0.10	51.4 ± 4.9
Y1 STA, TSA	9.77 ± 0.08	580 ± 170	9.01 ± 0.07	9.03 ± 0.26	58.2 ± 5.0
Y1 T356A, S359A, TSA	9.71 ± 0.08	500 ± 100	8.98 ± 0.06	9.21 ± 0.20	53.0 ± 7.4
Y1 5A	9.60 ± 0.06	440 ± 50	9.01 ± 0.15	8.81 ± 0.28	55.7 ± 3.4
Y1 6A	9.63 ± 0.02	340 ± 30	9.14 ± 0.22	9.04 ± 0.02	63.2 ± 1.2
Y2	11.10 ± 0.13	1190 ± 120	Not tested	9.19 ± 0.11	73.8 ± 3.5
Y2 H155P	11.03 ± 0.08	1440 ± 300	Not tested	9.17 ± 0.05	70.2 ± 5.3

All parameters were obtained from [^{125}I]PYY competition experiments as described in the Methods. In each case, maximal inhibition of [^{125}I]PYY specific binding was afforded by 1 μM GTPγS. Details of the various Y1 receptor mutations are given in the text.

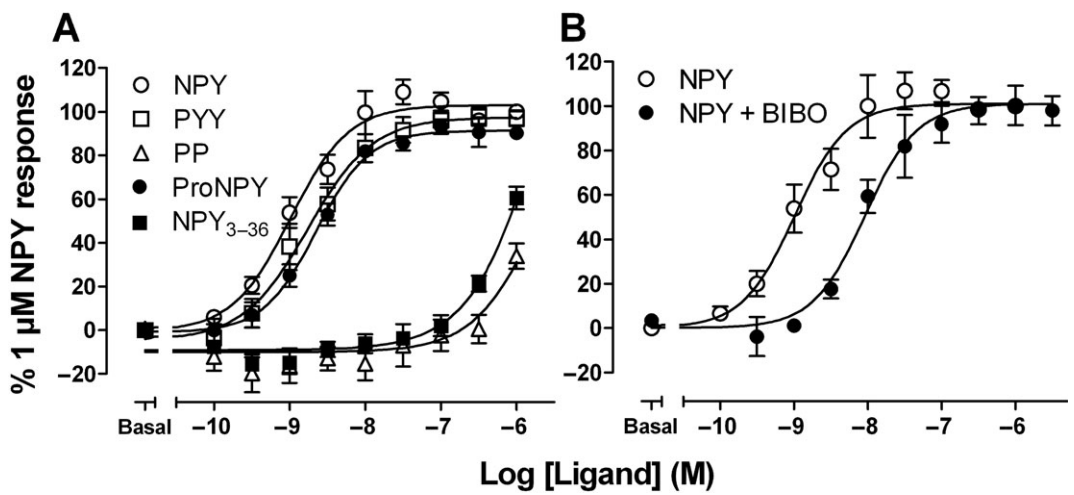

Figure 7 Agonist and antagonist data for human Y1 receptor stimulated β-arrestin2 BiFC. Human hY1/βarr2 cells were derived after further dilution cloning to optimize receptor and arrestin construct expression. The similarity with rat Y1/βarr2 cell data is illustrated by agonist concentration–response curves in (A), for 60 min treatment with NPY (pEC$_{50}$: 8.99 ± 0.08, *n* = 7), PYY (pEC$_{50}$: 8.76 ± 0.09, *n* = 6), PP (*n* = 6), [Leu^{31}, Pro^{34}]NPY (ProNPY pEC$_{50}$: 8.65 ± 0.06, *n* = 7) and NPY$_{3–36}$ (*n* = 6). In (B), 30 min pre-incubation with 10 nM BIBO3304 (BIBO) resulted in a 9.1-fold rightward shift in the NPY concentration–response relationship (*n* = 5) from which a pK$_B$ of 8.9 was calculated.

Reduced affinity of Y2 receptors for β-arrestin2 is revealed by the BiFC assay

Finally, we studied whether BiFC measurement of β-arrestin2 association could be applied to the human Y2 receptor, a subtype that also binds NPY and PYY, but is reported to recruit β-arrestin2 much less efficiently (Berglund *et al.*, 2003; Marion *et al.*, 2006). Receptor expression levels were slightly higher in the Y2–Yc/βarr2–Yn clone compared to Y1/βarr2 cells, with increased affinity for PYY (Table 2). Nevertheless, NPY, and to a lesser extent PYY, were significantly less potent agonists for stimulating Y2/βarr2 BiFC (Figure 10; Table 3) than observed for Y1/βarr2 responses (19-fold difference comparing NPY EC$_{50}$ values; $P < 0.001$). In Y2/βarr2 cells, [Leu^{31}, Pro^{34}]NPY was inactive (up to 1 μM) while the C-terminal fragment PYY$_{3–36}$ was a full agonist as potent as PYY (pEC$_{50}$ 7.71 ± 0.10, *n* = 4). H155P substitution in the Y2 receptor second intracellular loop has been reported to increase receptor affinity for β-arrestin2 (Marion *et al.*, 2006). Despite equivalent levels of receptor expression (Table 2), Y2H155P/βarr2 cells exhibited significantly increased basal and agonist-stimulated BiFC responses (Figure 10B). This was accompanied by a marked increase in potency for the agonists NPY and PYY (pEC$_{50}$s in Table 3), and for PYY$_{3–36}$ (pEC$_{50}$ 8.60 ± 0.22, *n* = 4).

Discussion

Here, we have described the use of BiFC to report the direct molecular association between typical 7TMRs (the Y1 or Y2 NPY receptors) and β-arrestin2. We used automated image analysis to quantify BiFC fluorescence readouts within individual cells in an unbiased manner, although other methods are also possible (Morell *et al.*, 2007). As for all 7TMR–β-arrestin assays, there were both advantages and limitations to the BiFC technique. However, the BiFC assay was able to provide quantitative ligand pharmacology and insight into

Table 3 Effect of Y1 and Y2 mutations on agonist potency and maximum response in the β-arrestin2 BiFC assay

Receptor	*NPY*		*PYY*	
	pEC_{50}	*1 μM response*	*pEC_{50}*	*1 μM response*
Y1	8.57 ± 0.05	100	8.54 ± 0.06	98.6 ± 7.6
Y1 Y99A	–	13.0 ± 3.6***	Not tested	Not tested
Y1 ΔY346	–	13.4 ± 4.7***	Not tested	Not tested
Y1 STA	8.49 ± 0.12	58.1 ± 5.7***	8.60 ± 0.16	77.6 ± 4.2
Y1 T356A	8.81 ± 0.22	60.2 ± 4.7***	8.69 ± 0.19	67.9 ± 6.2*
Y1 S359A	8.56 ± 0.16	77.9 ± 8.8	8.45 ± 0.16	74.1 ± 13.4
Y1 TSA	8.59 ± 0.16	79.8 ± 10.8	8.76 ± 0.16	77.4 ± 7.8
Y1 STA, TSA	8.41 ± 0.23	34.8 ± 7.1***	8.58 ± 0.42	46.5 ± 5.5***
Y1 T356A, S359A, TSA	8.53 ± 0.18	34.3 ± 11.2***	8.34 ± 0.32	33.0 ± 9.5***
Y1 5A	–	14.2 ± 3.1***	–	8.7 ± 3.8***
Y1 6A	–	19.7 ± 14.2***	–	9.5 ± 13.5***
Y2	7.15 ± 0.08	100	7.82 ± 0.09	101.8 ± 3.3
Y2 H155P	8.05 ± 0.34*	175.9 ± 29.2*	8.79 ± 0.28*	168.2 ± 23.9*

Data are obtained from 4–10 experiments (see also concentration–response curves in Figures 8 and 10). pEC_{50}s are not quoted (–) in mutants where agonist responses were too small for accurate estimates. Some mutants also changed basal β-arrestin2 BiFC as shown in Figures 8 and 10.
*$P < 0.05$, ***$P < 0.001$ compared to values for the native Y receptor, using one-way ANOVA and Dunnett's post test (Y1 mutations) or unpaired Student's *t*-test (Y2 vs. Y2H155P).

the molecular mechanisms governing β-arrestin2 recruitment by NPY receptors. It distinguished Y receptor mutations predicted to alter recognition by β-arrestin activation or phosphorylation sensors. Moreover, it indicated that alternative arrangements of Ser/Thr residues in the Y1 receptor C tail can support β-arrestin2 association.

Current popular imaging methods use FRET/BRET to measure 7TMR–β-arrestin interactions (Angers *et al.*, 2000; Berglund *et al.*, 2003; Charest *et al.*, 2005; Hoffmann *et al.*, 2008). RET assays report real-time responses as soon as the proximity or orientation of the donor and acceptor fluorophores changes. However, the generation of BiFC requires a sufficiently sustained protein–protein interaction to allow Yn and Yc fragment refolding to take place, although the distance constraints for complementation appear similar to RET (<10 nm apart; Remy *et al.*, 1999). Overlapping fragments from venus YFP (Nagai *et al.*, 2002; Hu and Kerppola, 2003; MacDonald *et al.*, 2006) maximized refolding rates, and were successful in trapping acute Y receptor–β-arrestin2 recruitment. Lower incubation temperatures were also unnecessary, in contrast to BiFC experiments with standard YFP constructs (Hu *et al.*, 2002; Briddon *et al.*, 2008). The disadvantage of using rapidly refolding BiFC partners can be elevated self-association and background signal (Kerppola, 2008). Multiple negative controls using Y1 receptor or β-arrestin mutants demonstrated that the non-specific BiFC response was low. Clearly, specificity is aided by compartmentalization of cell surface receptors and cytoplasmic β-arrestin2 until a stimulus brings them together. As Yn/Yc refolding is not instantaneous, it also reduces inappropriate BiFC signals from non-specific 'bystander' interactions.

A granularity algorithm applied to confocal plate reader images measured the intensity of Y receptor–β-arrestin2 BiFC in perinuclear compartments of stable co-transfected cells. This demonstrated first that NPY-induced BiFC developed with slow irreversible kinetics. The contrast with more rapid and reversible Y1–YFP receptor internalization, itself a β-arrestin-mediated event (Holliday *et al.*, 2005; Ouedraogo *et al.*, 2008), provided convincing evidence that NPY stimulation formed new BiFC complexes, rather than altering the trafficking of pre-existing ones. Thus, the BiFC assay is not a real-time indicator of β-arrestin2 recruitment. Fast refolding commits the complex to produce a fluorescent signal (Figure 1), but detection is artificially delayed by slow cYFP maturation (half-time ~50 min *in vitro*; Hu *et al.*, 2002). Conceivably, this process could influence agonist potency, for example, if the affinities of Yn and Yc for each other made a contribution to Y receptor–β-arrestin2 binding. Different lines of evidence demonstrate that this is not the case. First, NPY potencies did not change with incubation time, suggesting that longer stimulation increased only the proportion of refolded cYFP that matured and became fluorescent. Comparison of different peptide agonists, including Pro^{34} substituted analogues and 3–36 fragments (Michel *et al.*, 1998), provided the expected orders of potencies for Y1 or Y2 receptor-stimulated β-arrestin2 BiFC. For Y1 receptor responses, there was also a close correspondence with equivalent measurements for a dependent process, namely Y1–YFP internalization. The lower β-arrestin2 affinity of Y2 compared to Y1 receptors, originally evident from BRET measurements (Berglund *et al.*, 2003), was maintained in the BiFC assay. Most significantly, the affinities of Yn and Yc for each other could be adjusted by using different BiFC pairs, but this choice only influenced the kinetics of the Y1 receptor–β-arrestin2 response, and not agonist potency. We conclude that the BiFC approach provides reliable potency estimates for agonist-stimulated β-arrestin2 recruitment by Y receptors.

Our data support the consensus that in reforming the stable YFP β-barrel structure, BiFC generates an irreversible complex (Hu *et al.*, 2002; Morell *et al.*, 2007; Kerppola, 2008). This has practical advantages in comparison to RET methods, in that the response is sustained and less dependent on the time of measurement. However, the stability of 7TMR–β-arrestin complexes, as well as initial association, is functionally important (Gurevich and Gurevich, 2006; Tilley *et al.*, 2009). The lifetime of β-arrestin interaction can depend on the 7TMR inves-

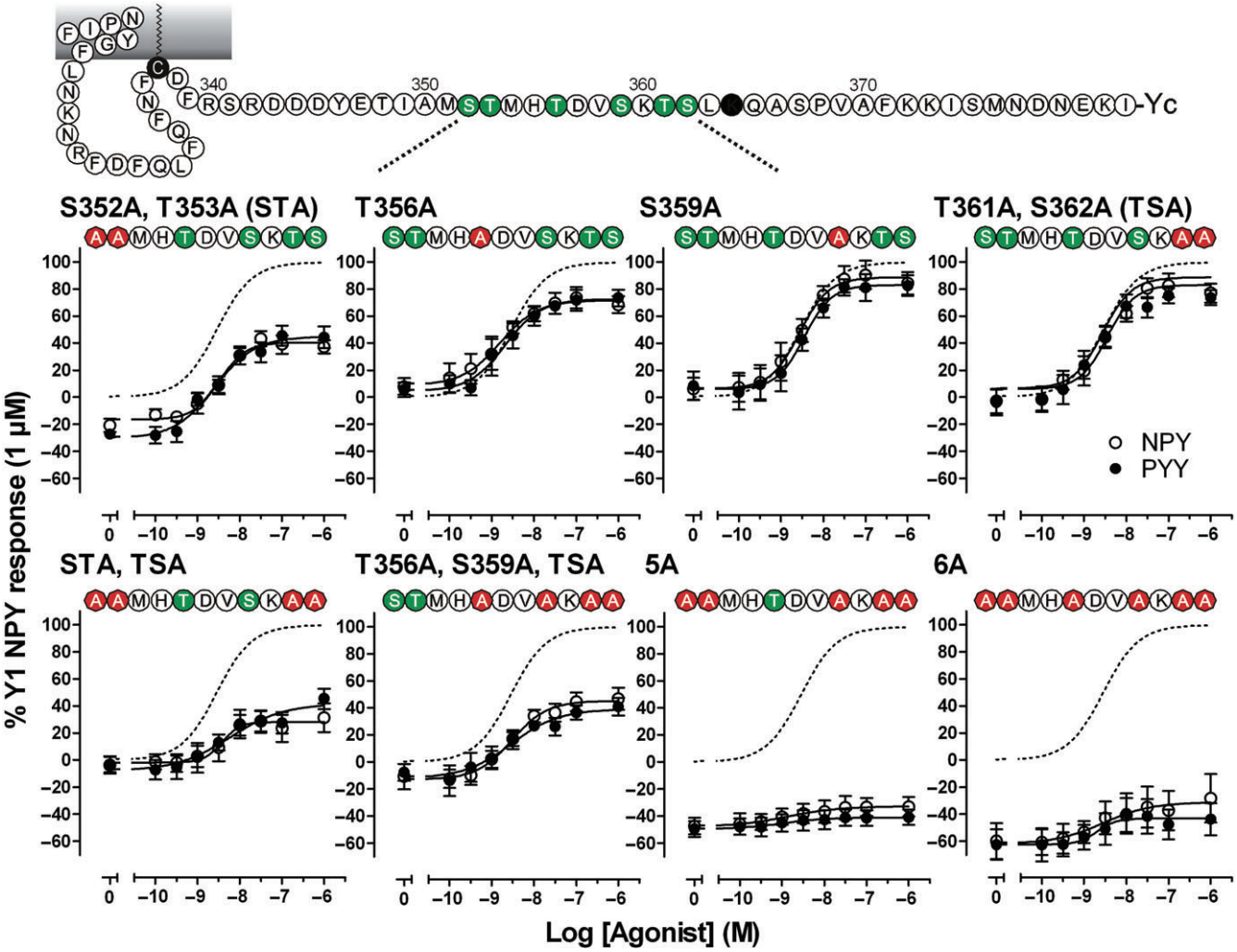

Figure 8 Mutating Y1 receptor C tail phosphorylation sites inhibits β-arrestin2 association. The upper diagram shows the C-terminal amino acid sequence of the rat Y1 receptor, highlighting the region between positions 352 and 362, which contains six Ser/Thr residues (white text on green) and which was identified previously as the key phosphorylated sequence in the receptor (Holliday *et al.*, 2005). These Ser/Thr residues were mutated individually or in combination, and eight stable Y1 mutant/βarr2 cell lines established with closely matched expression levels to Y1/βarr2 cells (Table 2). NPY- and PYY-stimulated β-arrestin2 BiFC responses were measured for each mutant and normalized by comparison with basal and 1 µM NPY Y1/βarr2 control responses on the same plate. Each graph presents the pooled data (n = 4–5) with the location of the Ala substitutions (white text on red) highlighted in the diagram above (STA = S352A, T353A; TSA = T361A, S362A; 5A = S352A, T353A, S359A, T361A, S362A; 6A = S352A, T353A, T356A, S359A, T361A, S362A). In each case, the dotted curve represents the NPY concentration–response curve for Y1/βarr2 cells (as Figure 5B). The curve fits yielded the pEC_{50} estimates in Table 3.

tigated (Oakley *et al.*, 2000; Hoffmann *et al.*, 2008), or on the nature of the ligand which activates a single 7TMR (Hoffmann *et al.*, 2008). Although the Y1 receptor promotes sustained endosomal recruitment of β-arrestin (Holliday *et al.*, 2005), the β-arrestin2 BiFC assay can equally be applied to the β_2-adrenoceptor which associates transiently with β-arrestin at the plasma membrane (Oakley *et al.*, 2000; Auld *et al.*, 2006; MacDonald *et al.*, 2006; D. Lake and N. Holliday, unpubl. obs.). However, the absence of BiFC dissociation is a limitation for assessing how ligands stabilize 7TMR–β-arrestin interaction, although more sustained complexes would enhance the probability of Yn/Yc fragment refolding. Subsequent signalling and intracellular trafficking of the stable BiFC complex may also be atypical, for example, because the fluorescent 7TMR–β-arrestin fusion protein created by BiFC impedes recycling (Oakley *et al.*, 1999). This difference was not obvious in our studies because both internalized Y1–YFP receptors and Y1 receptor–β-arrestin2 BiFC complexes accumulated in similar perinuclear compartments.

The Y1 receptor–β-arrestin2 BiFC assay demonstrated that BIBP3226 and BIBO3304 were competitive antagonists, with affinity estimates consistent with those from other studies (Michel *et al.*, 1998; Wieland *et al.*, 1998). GR231118 did not stimulate Y1 receptor internalization, in contrast to a previous report (Pheng *et al.*, 2003), and it was an antagonist for Y1 receptor–β-arrestin2 interaction (as in other functional assays; Michel *et al.*, 1998). Steep GR231118 Schild plots may indicate slow antagonist dissociation and conditions which do not approach equilibrium (Christopoulos *et al.*, 1999), rather than an inherent behaviour of the BiFC assay. No antagonist altered BiFC alone, but while this eliminates biased efficacy towards β-arrestin2 recruitment, it does not exclude possible

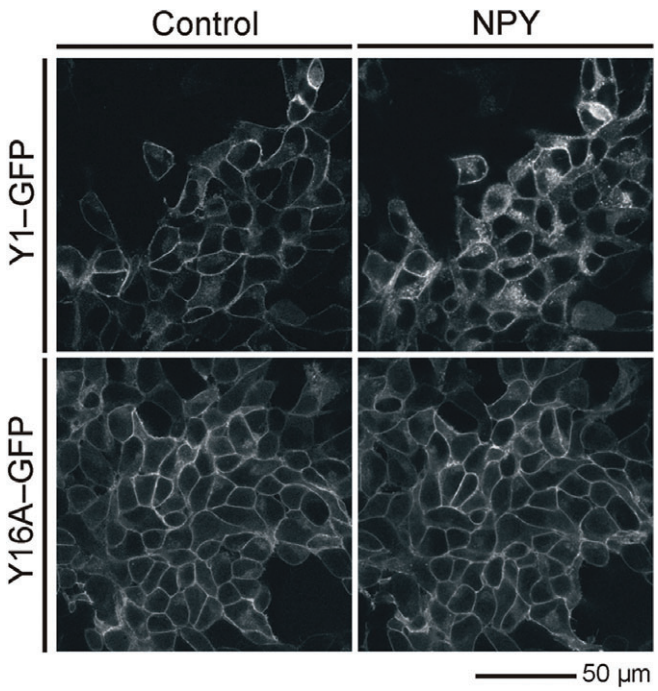

Figure 9 Phosphorylation site mutation prevents ligand and Y1 receptor internalization. 293TR Y1-GFP and Y16A-GFP cells (with all six Ser/Thr substituted between Ser352 and S362) were treated with tetracycline (1 μg·mL^{-1}) for 21 h to induce receptor expression. Confocal images were acquired from living cells before ligand addition, or 15 min after treatment with 1 μM NPY. Example images are representative of three experiments.

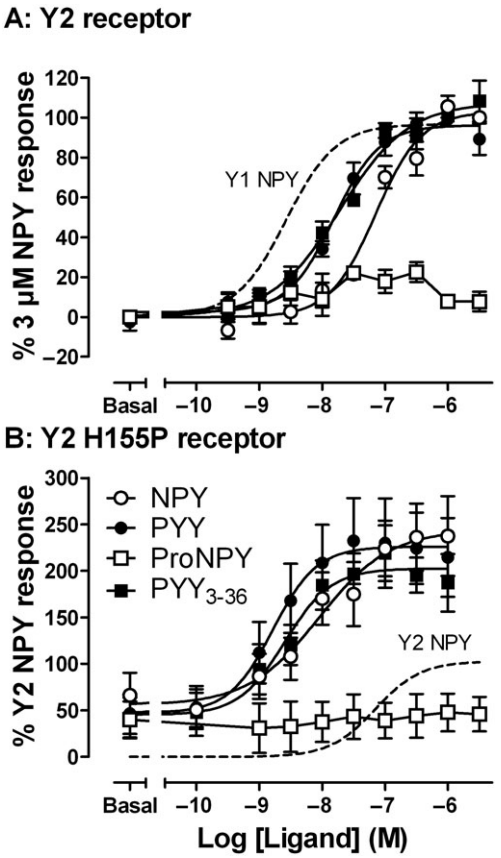

Figure 10 Y2 receptor–β-arrestin2 interaction and its restoration by H155P substitution. Concentration–response curves from pooled analysis data (vesicle intensity/cell; n = 4–6 experiments) show agonist-stimulated β-arrestin2 BiFC in stably transfected cells expressing Yc-tagged Y2 receptors (A) or the Y2H155P mutant (B). Both Y2/β-arr2 and Y2H155P/β-arr2 cells expressed similar numbers of receptors (Table 2), and Y2H155P/β-arr2 BiFC responses were normalized with reference to Y2/β-arr2 controls in each experimental plate. Dotted curves illustrate the positions of the Y1/β-arr2 (A) or Y2/β-arr2 (B) NPY concentration–response curves for comparison. ProNPY is [Leu^{31}, Pro^{34}]NPY.

inverse agonist properties. Pre-existing stable Y1 receptor–β-arrestin2 cYFP complexes would be resistant to ligand-induced dissociation. In principle, inverse agonists might effect a change by preventing constitutive association of new complexes, but this is unlikely to be detected with acute incubations.

Recognition of agonist-occupied and phosphorylated 7TMRs requires distinct molecular determinants within β-arrestins. First, the positive β-arrestin residues form new salt bridges with phosphorylated or acidic residues in intracellular 7TMR domains. Disruption of the β-arrestin 'polar core' promotes conformational rearrangement to a state more capable of binding activated 7TMRs (Gurevich and Gurevich, 2006). Within a previously identified phosphorylated region of the Y1 receptor C tail (Holliday *et al.*, 2005), sequential Ala substitution of the six Ser/Thr residues presents decreased maximum β-arrestin2 binding without altering agonist potency in the BiFC assay. This befits mutations which affect the phosphate 'trigger', rather than changing the discrimination by β-arrestin between empty and agonist-occupied receptors. Surprisingly, the number of phosphorylation site mutations (4/6 for substantive inhibition) proved to be more important than their precise location. Thus, while one inhibitory 4/6 mutant was equivalent to a previously reported critical binding motif (T356A, S359A, TSA; Ouedraogo *et al.*, 2008), a second set of 4/6 substitutions (STA, TSA) was equally effective. Mutating the two remaining Ser/Thr was then necessary to eliminate β-arrestin2 binding and internalization. Both 5A and 6A mutants also reduced basal β-arrestin2 BiFC, suggesting some constitutive Y1 receptor–β-arrestin2 interaction, at least in transfected cells. This is consistent with some basal Y1 receptor internalization identified by the live antibody labelling technique (Holliday *et al.*, 2005), particularly when β-arrestin2 is co-transfected (Figure 2).

The apparent redundancy in the exact phosphorylation sites required for Y1 receptor–β-arrestin interaction concurs with studies using rhodopsin (Doan *et al.*, 2006) and chemokine receptor 5 (Huttenrauch *et al.*, 2002), although a more complex interplay is also possible (Gurevich and Gurevich, 2006; Potter *et al.*, 2006; Tobin *et al.*, 2008). One implication from the 4/6 mutants is that alternative arrangements of Y1 receptor phosphorylated residues can support some β-arrestin2 interaction, consistent with a required cluster of only two to three negative charges for β-arrestin binding (Huttenrauch *et al.*, 2002; Gurevich and Gurevich, 2006). Intriguingly, this might confer distinct active β-arrestin conformations, as proposed recently (Tobin *et al.*, 2008; Zidar *et al.*, 2009).

The second arrestin binding element recognizes activated 7TMRs, via less well-defined receptor motifs (Huttenrauch

et al., 2002; Marion *et al.*, 2006). One is a conserved proline-containing sequence following the DRY motif in intracellular loop 2. Its restoration by H155P substitution in the Y2 receptor increases β-arrestin interaction (Marion *et al.*, 2006). Interestingly, this mutant not only enhanced the size of the Y2 receptor–β-arrestin2 BiFC response, but significantly increased agonist potency, contrasting with potency-independent actions of phosphorylation site mutants. Thus, mutations which affect binding via the arrestin activation or phosphorylation sensors display different characteristics in the BiFC assay.

Various other approaches quantify recruitment of β-arrestins to 7TMRs, each with its own advantages and pitfalls. Other complementation methods include the restoration of β-galactoside enzyme activity when 7TMRs and β-arrestin associate (Carter and Hill, 2005). A second assay (TANGO, Invitrogen; Hanson *et al.*, 2009) requires the engineered release of a transcription factor from the receptor on β-arrestin binding, which then activates a downstream β-lactamase reporter for assay. In both cases, detection is straightforward in fixed or lysed cells, but each requires addition of enzyme substrate, with no information on response localization. The direct correspondence of BiFC with molecular 7TMR–β-arrestin interaction, and its applicability to living cells, is best replicated by RET methods, or measurement of β-arrestin–GFP translocation to unmodified 7TMRs (Hudson *et al.*, 2006). Here, the stability of the generated BiFC response in living cells (in contrast to transient translocation or RET responses) could actually offer a practical advantage for high-content imaging purposes. All current β-arrestin assays, including BiFC, share the limitation of their restriction to recombinant cell systems, using transfected and modified 7TMR or β-arrestin proteins. Care must be taken in extrapolating these results to the pharmacology and function of native 7TMRs in their physiological context. For example, the profile and sites of 7TMR phosphorylation, which drives β-arrestin recruitment, can differ significantly between standard cell lines and native cells (Tobin *et al.*, 2008). We have shown that the 7TMR–β-arrestin2 assay can, in principle, be performed in primary smooth muscle cells (N. Holliday, unpubl. obs.); while this still requires recombinant proteins and transfection, it should allow future investigations in a more physiological cell environment.

The use of BiFC to study signalling is at an early stage, but has significant potential because of the simplicity and range of measurements possible in living cells (MacDonald *et al.*, 2006; Kerppola, 2008; Rose *et al.*, 2010). Here, we have shown that this approach delivers robust quantitative pharmacology focused on the molecular interaction between 7TMRs and β-arrestin2. BiFC can be expanded in combination with BRET (Gandia *et al.*, 2008) or in multicolour assays (Mervine *et al.*, 2006) to examine co-operative or competitive multi-component interactions. These present future opportunities to put 7TMR–β-arrestin recruitment into the context of the multi-protein signalling complexes it creates.

Acknowledgements

We would like to thank Dr F. Ciruela (University of Barcelona) for providing the original YFP constructs, Dr H. Doods (Boehringer-Ingelheim, Rhein, Germany) for the gift of BIBO3304 and David Lake (NDH's laboratory) for critical reading of the manuscript. This work was supported by the Medical Research Council Grant G0700049, to N.D.H., S.J.B. and S.J.H.

Conflict of interest

The authors declare they have no conflicts of interest.

References

Alexander SPH, Mathie A, Peters JA (2009). *Guide to Receptors and Channels (GRAC)*, 4th edn. *Br J Pharmacol* **158** (Suppl. 1): S1–S254.

Angers S, Salahpour A, Joly E, Hilairet S, Chelsky D, Dennis M *et al.* (2000). Detection of beta 2-adrenergic receptor dimerization in living cells using bioluminescence resonance energy transfer (BRET). *Proc Natl Acad Sci USA* **97**: 3684–3689.

Auld DS, Johnson RL, Zhang Y, Veith H, Jadhav A, Yasgar A (2006). Fluorescent protein-based cellular assays analysed by laser-scanning microplate cytometry in 1536-well plate format. *Methods Enzymol* **414**: 566–589.

Azzi M, Charest PG, Angers S, Rousseau G, Kohout T, Bouvier M *et al.* (2003). Beta-arrestin-mediated activation of MAPK by inverse agonists reveals distinct active conformations for G protein-coupled receptors. *Proc Natl Acad Sci USA* **100**: 11406–11411.

Baker JG, Hall IP, Hill SJ (2003). Agonist and inverse agonist actions of beta-blockers at the human beta 2-adrenoceptor provide evidence for agonist-directed signaling. *Mol Pharmacol* **64**: 1357–1369.

Baldock PA, Allison SJ, Lundberg P, Lee NJ, Slack K, Lin EJ *et al.* (2007). Novel role of Y1 receptors in the coordinated regulation of bone and energy homeostasis. *J Biol Chem* **282**: 19092–19102.

Berglund MM, Schober DA, Statnick MA, McDonald PH, Gehlert DR (2003). The use of bioluminescence resonance energy transfer 2 to study neuropeptide Y receptor agonist-induced beta-arrestin 2 interaction. *J Pharmacol Exp Ther* **306**: 147–156.

Briddon SJ, Gandia J, Amaral OB, Ferre S, Lluis C, Franco R *et al.* (2008). Plasma membrane diffusion of G protein-coupled receptor oligomers. *Biochim Biophys Acta* **1783**: 2262–2268.

Carter AA, Hill SJ (2005). Characterization of isoprenaline- and salmeterol-stimulated interactions between beta2-adrenoceptors and beta-arrestin 2 using beta-galactosidase complementation in C2C12 cells. *J Pharmacol Exp Ther* **315**: 839–848.

Charest PG, Terillon S, Bouvier M (2005). Monitoring agonist-promoted conformational changes of beta-arrestin in living cells by intramolecular BRET. *EMBO Rep* **6**: 334–340.

Christopoulos A, Parsons AM, Lew MJ, El-Fakahany EE (1999). The assessment of antagonist potency under conditions of transient response kinetics. *Eur J Pharmacol* **382**: 217–227.

Doan T, Mendez A, Detwiler PB, Chen J, Rieke F (2006). Multiple phosphorylation sites confer reproducibility of the rod's single-photon responses. *Science* **313**: 530–533.

Gandia J, Galino J, Amaral OB, Soriano A, Lluis C, Franco R *et al.* (2008). Detection of higher-order G protein-coupled receptor oligomers by a combined BRET–BiFC technique. *FEBS Lett* **582**: 2979–2984.

Gurevich VV, Gurevich EV (2006). The structural basis of arrestin-mediated regulation of G-protein-coupled receptors. *Pharmacol Ther* **110**: 465–502.

Hanson BJ, Wetter J, Bercher MR, Kopp L, Vedvik KL, Zielinski T *et al.* (2009). A homogeneous fluorescent live-cell assay for measuring 7-transmembrane receptor activity and agonist functional selectivity through beta-arrestin recruitment. *J Biomol Screen* **14**: 798–810.

Hoffmann C, Ziegler N, Reiner S, Krasel C, Lohse MJ (2008). Agonist-selective, receptor-specific interaction of human P2Y receptors with beta-arrestin-1 and -2. *J Biol Chem* **283**: 30933–30941.

Holliday ND, Lam CW, Tough IR, Cox HM (2005). Role of the C terminus in neuropeptide Y Y1 receptor desensitization and internalization. *Mol Pharmacol* **67**: 655–664.

Hu CD, Kerppola TK (2003). Simultaneous visualization of multiple protein interactions in living cells using multicolor fluorescence complementation analysis. *Nat Biotechnol* **21**: 539–545.

Hu CD, Chinenov Y, Kerppola TK (2002). Visualization of interactions among bZIP and Rel family proteins in living cells using bimolecular fluorescence complementation. *Mol Cell* **9**: 789–798.

Hudson CC, Oakley RH, Sjaastad MD, Loomis CR (2006). High-content screening of known G protein-coupled receptors by arrestin translocation. *Methods Enzymol* **414**: 63–78.

Huttenrauch F, Nitzki A, Lin FT, Honing S, Oppermann M (2002). Beta-arrestin binding to CC chemokine receptor 5 requires multiple C-terminal receptor phosphorylation sites and involves a conserved Asp-Arg-Tyr sequence motif. *J Biol Chem* **277**: 30769–30777.

Karra E, Chandarana K, Batterham RL (2009). The role of peptide YY in appetite regulation and obesity. *J Physiol* **587**: 19–25.

Kerppola TK (2008). Bimolecular fluorescence complementation (BiFC) analysis as a probe of protein interactions in living cells. *Annu Rev Biophys* **37**: 465–487.

MacDonald ML, Lamerdin J, Owens S, Keon BH, Bilter GK, Shang Z *et al*. (2006). Identifying off-target effects and hidden phenotypes of drugs in human cells. *Nat Chem Biol* **2**: 329–337.

Marion S, Oakley RH, Kim KM, Caron MG, Barak LS (2006). A beta-arrestin binding determinant common to the second intracellular loops of rhodopsin family G protein-coupled receptors. *J Biol Chem* **281**: 2932–2938.

Mervine SM, Yost EA, Sabo JL, Hynes TR, Berlot CH (2006). Analysis of G protein betagamma dimer formation in live cells using multicolor bimolecular fluorescence complementation demonstrates preferences of beta1 for particular gamma subunits. *Mol Pharmacol* **70**: 194–205.

Michel MC, Beck-Sickinger A, Cox H, Doods HN, Herzog H, Larhammar D *et al*. (1998). XVI. International Union of Pharmacology recommendations for the nomenclature of neuropeptide Y, peptide YY, and pancreatic polypeptide receptors. *Pharmacol Rev* **50**: 143–150.

Morell M, Espargaro A, Aviles FX, Ventura S (2007). Detection of transient protein–protein interactions by bimolecular fluorescence complementation: the Abl-SH3 case. *Proteomics* **7**: 1023–1036.

Nagai T, Ibata K, Park ES, Kubota M, Mikoshiba K, Miyawaki A (2002). A variant of yellow fluorescent protein with fast and efficient maturation for cell-biological applications. *Nat Biotechnol* **20**: 87–90.

Nelson CD, Perry SJ, Regier DS, Prescott SM, Topham MK, Lefkowitz RJ (2007). Targeting of diacylglycerol degradation to M1 muscarinic receptors by beta-arrestins. *Science* **315**: 663–666.

Oakley RH, Laporte SA, Holt JA, Barak LS, Caron MG (1999). Association of beta-arrestin with G protein-coupled receptors during clathrin-mediated endocytosis dictates the profile of receptor resensitization. *J Biol Chem* **274**: 32248–32257.

Oakley RH, Laporte SA, Holt JA, Caron MG, Barak LS (2000). Differential affinities of visual arrestin, beta arrestin1, and beta arrestin2 for G protein-coupled receptors delineate two major classes of receptors. *J Biol Chem* **275**: 17201–17210.

Ouedraogo M, Lecat S, Rochdi MD, Hachet-Haas M, Matthes H, Gicquiaux H *et al*. (2008). Distinct motifs of neuropeptide Y receptors differentially regulate trafficking and desensitization. *Traffic* **9**: 305–324.

Perry SJ, Baillie GS, Kohout TA, McPhee I, Magiera MM, Ang KL *et al*. (2002). Targeting of cyclic AMP degradation to beta 2-adrenergic receptors by beta-arrestins. *Science* **298**: 834–836.

Pheng LH, Dumont Y, Fournier A, Chabot JG, Beaudet A, Quirion R (2003). Agonist- and antagonist-induced sequestration/internalization of neuropeptide Y Y1 receptors in HEK293 cells. *Br J Pharmacol* **139**: 695–704.

Potter RM, Maestas DC, Cimino DF, Prossnitz ER (2006). Regulation of *N*-formyl peptide receptor signaling and trafficking by individual carboxyl-terminal serine and threonine residues. *J Immunol* **176**: 5418–5425.

Remy I, Wilson IA, Michnick SW (1999). Erythropoietin receptor activation by a ligand-induced conformation change. *Science* **283**: 990–993.

Rose RH, Briddon SJ, Holliday ND (2010). Bimolecular fluorescence complementation: lighting up seven transmembrane domain receptor signalling networks. *Br J Pharmacol* **159**: 738–750.

Sjodin P, Holmberg SK, Akerberg H, Berglund MM, Mohell N, Larhammar D (2006). Re-evaluation of receptor–ligand interactions of the human neuropeptide Y receptor Y1: a site-directed mutagenesis study. *Biochem J* **393**: 161–169.

Tilley DG, Kim IM, Patel PA, Violin JD, Rockman HA (2009). β-Arrestin mediates β1-adrenergic receptor–epidermal growth factor receptor interaction and downstream signaling. *J Biol Chem* **284**: 20375–20386.

Tobin AB, Butcher AJ, Kong HC (2008). Location, location, location . . . site-specific GPCR phosphorylation offers a mechanism for cell-type-specific signalling. *Trends Pharmacol Sci* **29**: 413–420.

Vidi PA, Chen J, Irudayaraj JM, Watts VJ (2008). Adenosine A(2A) receptors assemble into higher-order oligomers at the plasma membrane. *FEBS Lett* **582**: 3985–3990.

Wieland HA, Engel W, Eberlein W, Rudolf K, Doods HN (1998). Subtype selectivity of the novel nonpeptide neuropeptide Y Y1 receptor antagonist BIBO 3304 and its effect on feeding in rodents. *Br J Pharmacol* **125**: 549–555.

Zidar DA, Violin JD, Whalen EJ, Lefkowitz RJ (2009). Selective engagement of G protein coupled receptor kinases (GRKs) encodes distinct functions of biased ligands. *Proc Natl Acad Sci USA* **106**: 9649–9654.

Supporting information

Additional Supporting Information may be found in the online version of this article:

Figure S1 NPY-stimulated Y1 receptor/β-arrestin2 BiFC in live stably transfected HEK293 cells. The Y1/βarr2 clone was incubated in the absence or presence of 1 μM NPY (60 min, 37°C) before acquiring confocal BiFC fluorescence and phase images under identical settings.

Figure S2 Granularity algorithm to quantify Y1–YFP internalization. Automated plate reader images illustrate NPY-(100 nM, 15 min) induced endocytosis of Y1 receptors labelled with Y1vYFP (A). Below, granularity analysis identifies internalized receptors based on the same-sized vesicles as for BiFC (3 μm + diameter, white dots), and H33342 stained nuclei (not shown). Detection of plasma membrane Y1–YFP fluorescence was minimized because of the size and intensity constraints for classification. As for BiFC analysis (Figure 3), this enabled construction of NPY concentration–response curves ($n = 5$) for vesicle count and average intensity/cell (B). The NPY pEC_{50} value from intensity data is in Table 1.

Please note: Wiley-Blackwell are not responsible for the content or functionality of any supporting materials supplied by the authors. Any queries (other than missing material) should be directed to the corresponding author for the article.